

## A Schottky-Diode Model of the Nonlinear Insulation Resistance in HTSPRTs—Part II: Detailed Two- and Three-Wire Measurements

K. Yamazawa · M. Arai · D. R. White

Published online: 9 October 2007  
© Springer Science+Business Media, LLC 2007

**Abstract** Electrical leakage is a significant factor in the uncertainty of temperature measurements employing high-temperature standard platinum-resistance thermometers, with effects as large as several millikelvin at the freezing point of silver (962°C). The insulation resistance also exhibits complex behavior that includes non-linearities, sensitivity to the electrical environment, and the generation of spurious voltages and currents. In an earlier article, it was suggested that the behavior is consistent with the existence of metal–semiconductor diodes, also known as Schottky-barrier or point-contact diodes, formed at the points of contact between platinum wire and fused-silica insulators supporting the platinum. In this article, we describe detailed measurements of the non-linear resistance of a fused-silica insulator supported by platinum wires. The discussion includes a detailed description of the measurement system, and the results of two experiments that show many of the features suggested by the metal–semiconductor-diode model. Observed features in the current–voltage measurements include an S-shaped feature characteristic of back-to-back diodes, temperature dependence of saturation currents consistent with thermionic emission, and a diode polarity consistent with silica being a p-type semiconductor. Some impacts of the model on thermometry practice are also noted.

**Keywords** Electrical insulation · Leakage effect · Nonlinear · Platinum resistance thermometer · Schottky diode

---

K. Yamazawa (✉) · M. Arai  
National Metrology Institute of Japan (NMIJ), AIST Tsukuba Central 3, 1-1-1 Umezono,  
Tsukuba Ibaraki 305-8563, Japan  
e-mail: kazuaki-yamazawa@aist.go.jp

D. R. White  
Measurement Standards Laboratory of New Zealand (MSL), P.O. Box 31310, Lower Hutt 5040  
New Zealand

## 1 Introduction

Electrical leakage is a well-known and significant factor in the uncertainty of temperature measurements employing high-temperature standard platinum-resistance thermometers (HTSPRTs) [1–7]. Even with sensing resistances as low as  $0.25\ \Omega$  at  $0.01^\circ\text{C}$ , effects may be as large as several millikelvin at the freezing point of silver ( $962^\circ\text{C}$ ). The simplest and most broadly accepted equivalent electrical circuit has an insulating resistance that is in parallel with the sensor resistance, and decreases with increasing temperature, causing a bias in temperature measurements. Some attempts to establish a more detailed model of the leakage effect exist in the literature. However, as Berry first showed [3, 4] and others have confirmed [5–7], the leakage effect is not a simple phenomenon. Berry introduced a model with a local ‘insulation battery’ effect to explain his findings. However, the cause of this insulation battery effect remains unexplained.

In an accompanying article [8], we suggested that the nonlinear insulation resistance effects at high temperatures can be explained by metal–semiconductor diodes, also known as point-contact or Schottky-barrier diodes, formed at the points of contact between the fused silica insulators and platinum of the SPRT sensing element and lead wires. Both crystalline (quartz) and fused silica should be very good insulators with energy band gaps of approximately 8–9 eV. However, impurity states with energy levels within the band gap change its electronic characteristics, and when the silica is exposed to high temperatures, it becomes an extrinsic semiconductor. In this condition, each contact between the metal and the silica insulator forms a Schottky-barrier diode. Thus, for example, the equivalent circuit of a single silica insulator connected to two platinum wires should include two back-to-back diodes.

In this article, we describe detailed measurements of the nonlinear resistance of the fused-silica insulators used in HTSPRTs in order to confirm the Schottky-barrier model. In Sect. 2, we first describe the measurement system and some evaluations of its performance. Sections 3 and 4 describe the design, measurement results, and analyses of the two experiments, which show many of the features predicted by the model. Finally, we draw some conclusions, and suggest some possibilities for improvements to the methods for estimating uncertainty due to insulation effects, and for the development of better HTSPRTs.

## 2 Experimental Apparatus

### 2.1 Electrical Measurements

The aim of the two experiments described below is to measure the current–voltage ( $I - V$ ) characteristics of devices expected to have distinctive non-linearities below 1 V, and resistances in the range from  $10\ \text{M}\Omega$  to  $20\ \text{G}\Omega$ . In order to elucidate the characteristics of the electrical insulation within platinum resistance thermometers, the range of applied voltages should include the voltages typically used in platinum resistance thermometry, i.e., below  $\pm 0.1\ \text{V}$ . The low voltages required, mean that commercial

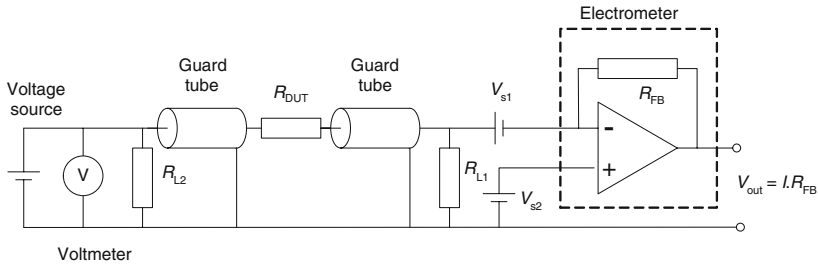


**Fig. 1** An equivalent circuit for the electrical measurement.  $R_{L1}$  and  $R_{L2}$  are unwanted leakage resistances;  $V_{s1}$  and  $V_{s2}$  are unwanted stray voltages

insulation-resistance meters are unsuited to the task, as they often apply voltages in the range from 100 to 1,000 V.

Another requirement for the measurement system is that it should not influence the apparent characteristics of the device under test (DUT). This means that consideration must be given to the input impedances of voltmeters and current meters. In particular, since most digital multimeters measure current by measuring the voltage drop across a series resistor, the presence of the meter can reduce the voltage across the DUT.

After considering various approaches, we have adopted a method employing a controllable voltage source and an electrometer [9]. This makes it possible to obtain a high resolution in voltage, to eliminate the effects of leakage resistances, and to eliminate the effects of finite input impedances of the meters. A simplified schematic diagram of the electrical measurement is shown in Fig. 1. The instruments used are a Keithley Model 2010 digital multimeter, a Keithley Model 6517A electrometer, and a Yokogawa Model 7651 programmable voltage source.

The key feature of the measurement system is that the measured current is minimally affected by a variety of leakage resistances. The electrometer, by applying negative feedback for the internal amplifier, ensures that the input of the electrometer is at 0 V. This then ensures that the leakage resistance  $R_{L1}$  has no current flowing through it, and therefore cannot affect the measurement. For the same reason, the finite input resistance of the electrometer has a negligible second-order effect. This insensitivity to leakage resistances is exploited further by completely surrounding the lead wires with alumina insulators and platinum tubes connected to the low potential lead. In this way, the measurement system eliminates leakage resistances to the leads. Further, the guard tubes also intercept leakage currents from outside the system (e.g., from furnace power supplies), and shunt the currents away from the electrometer.

At the other end of the measurement system, the leakage resistance  $R_{L2}$  and the finite input impedance of the voltmeter have no effect because the current passed by the resistor is not measured by the electrometer, and the low-impedance voltage source supplies as much current as required.

The measurement system is, however, susceptible to stray voltages causing a bias in the current measurements. As the equivalent circuit shows, the electrometer with its feedback resistor  $R_{FB}$ , in combination with the resistance of the DUT,  $R_{DUT}$ , ideally forms an amplifier with a non-inverting gain of  $1 + R_{FB}/R_{DUT}$ . In practice, the gain is a little larger because of the leakage resistance,  $R_{L1}$ . Thus, any stray voltages,  $V_{s1}$

and  $V_{s2}$ , emerging between the electrometer inputs and the guard tube are amplified, and this becomes increasingly apparent as the temperature rises and the value of  $R_{DUT}$  decreases. We found that the combination of stray voltages and varying leakage resistances was the main reason for irreproducibility in the electrometer readings. Since the guard tubes do not completely surround the DUT, there was also some remnant leakage current from the heater power source flowing into the leads near the DUT. Since these factors are intrinsic to the measurement system, we chose to offset readings using the bias measured when 0 V is applied to the DUT.

Upon assembling the electrical measurement components, we evaluated the  $I - V$  characteristics of standard resistors to confirm their capability. Four high-resistance standard resistors designed for use at voltages up to 1,000 V (10 T $\Omega$ , 100 G $\Omega$ , 1 G $\Omega$ , and 10 M $\Omega$ , Japan Hydrazine Co. Inc.) were used in the confirmation tests. By sweeping the applied voltage over  $\pm 10$  V, we evaluated the 20 pA, 200 pA, 2 nA, 20 nA, 200 nA, and 2  $\mu$ A ranges of the 6517A electrometer. In all measurements, the accuracy and linearity of the system was confirmed, with the slope obtained from the  $I - V$  characteristics coinciding with the nominal resistance value of the standard resistors within the uncertainties stated on the manufacturer's test report. The only departure from ideality was a negligible bias (approximately 0.2 pA, about 1%) observed in the 20 pA range measurements using the 10 T $\Omega$  resistors.

## 2.2 Furnace

The furnace used for the measurements was originally designed to anneal platinum resistance thermometers. The heater tube length is 600 mm long, and controlled by a feedback loop employing a Type R thermocouple for the sensor. In order to minimize the electrical noise, a series-regulated DC power supply is used, and the winding of the heater is designed to be non-inductive.

A 200 mm long SiC block with three bores is placed in the center of the heater tube as the isothermal block. The temperature distribution within the region 10 cm from the bottom of the wells was within  $\pm 1^\circ\text{C}$ .

During the  $I - V$  measurements, the specimen was placed in one well of the block within the isothermal region, while a second Type R thermocouple was placed in another well as a monitor. The temperature distribution inside the furnace reached equilibrium approximately 3 h after reaching the set temperature, and was stable within  $\pm 0.03^\circ\text{C}$ .

## 2.3 System Evaluation

To evaluate the complete measurement system and confirm the utility of the guarding structure, a blank specimen was made with the complete lead wire assembly, but no DUT, and measured at temperatures of 450, 700, 800, 900, and 1,000 $^\circ\text{C}$ . Figure 2 shows the results of the measurements. A bias in the current measurement started to appear at 800 $^\circ\text{C}$ , and increased as the temperature increased. However, the current bias was less than 100 pA at 800 $^\circ\text{C}$ , and was negligible compared to all measurements on actual samples. Also, an ohmic slope in the  $I - V$  curve appeared at 1,000 $^\circ\text{C}$ . The

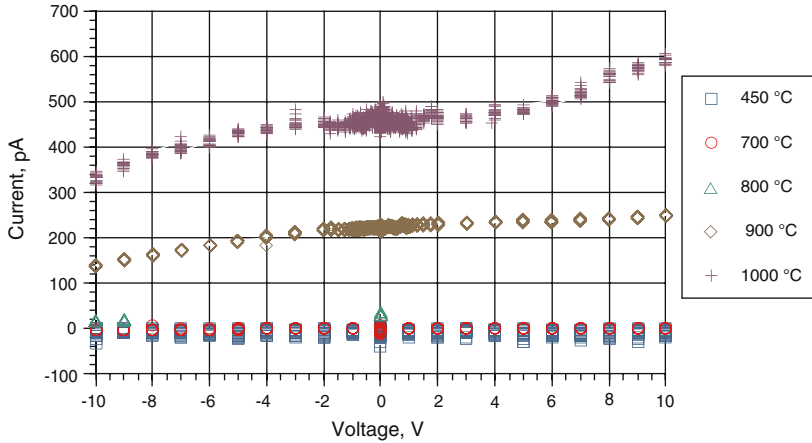


**Fig. 2**  $I - V$  characteristics of the measurement system as a function of test temperature, measured with the blank specimen

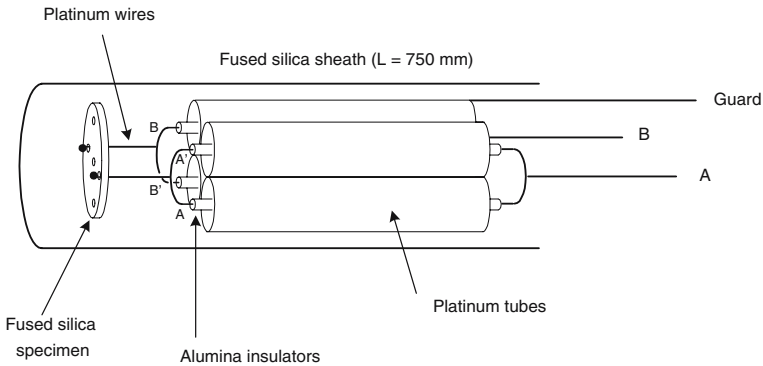


**Fig. 3** Structure of the holder with the specimen used in the two-wire experiment (Not to scale, details of the air-tight seal at the end of the silica sheath are not shown.)

implied resistance is above 50 GΩ, and is much higher than the resistance of the DUT at that temperature.

### 3 $I - V$ Characteristics of a Fused-silica Insulator

#### 3.1 Structure of the Specimen

The aim of this “two-wire” experiment was to reveal the  $I - V$  characteristics of platinum–silica points contact formed where two platinum lead wires are inserted through the holes of a fused-silica disc, and to verify the presence or absence of Schottky diodes at these points. Figure 3 shows the specimen holder and the specimen, with the two platinum leads inserted through the diagonal bore of the fused silica disk. The assembly is a four-wire system with separate guards for each wire, as outlined in

**Table 1** Nominal impurity composition of the fused-silica insulating disc [10]. Concentrations are given in parts-per-million by mass

Impurity	Concentration	Impurity	Concentration
Al	14	Mg	0.1
As	< 0.002	Mn	< 0.05
B	< 0.2	Na	0.7
Ca	0.4	Ni	< 0.1
Cd	< 0.01	P	< 0.2
Cr	< 0.05	Sb	< 0.003
Cu	< 0.05	Ti	1.1
Fe	0.2	Zr	0.8
K	0.6	+OH <sup>-</sup>	< 5
Li	0.5		

Sect. 2. For this experiment, the two pairs of leads were connected together (A–A' and B–B'). This arrangement provides some redundancy against a wire being broken by thermal expansion. Leads A and A' were connected to the voltage source, leads B and B' were connected to the electrometer, and the guards were connected to the guard point of the measurement circuit. The specimen and the guard structure were placed within a quartz sheath filled with dried air at a pressure of approximately 25 kPa at room temperature.

The disc for the specimen was supplied by Chino, and made from silica electrically fused under an inert gas environment. The disc is identical to those used in Chino's Standard Platinum Resistance Thermometer products. Table 1 summarizes the nominal impurities of the quartz material used for the specimen [10]. The disc is 5 mm in diameter with five 1 mm diameter holes, one in the center and four placed in a 2.8 mm diameter circle around the center. Platinum wires of 0.5 mm diameter were used for each lead. To ensure contact with the quartz specimen, the end of the lead was melted to form a ball of approximately 1.5 mm diameter, and the disc was held by these balls. Despite the redundant structure design described above, the length of each of the four leads was carefully adjusted, and also carefully treated to avoid any possibility of non-uniform thermal expansion that may result in change of the contact between the quartz and the platinum wire. All the parts of the assembly were cleaned first with ethanol, then rinsed by pure water, then with nitric acid, rinsing again carefully by pure water, and finally dried on a hot plate at 50°C. Special care was taken with the final rinse to remove all traces of the nitric acid.

### 3.2 Experimental Procedures

Measurements of the  $I - V$  characteristics were made at selected temperatures above 700°C, in a sequence from lower to higher temperatures. At each temperature setting, after waiting for the furnace to reach thermal equilibrium, we measured the  $I - V$  characteristics by applying voltages from  $-10$  V to 10 V, in the sequence from most negative to the most positive voltages. For each voltage setting, we measured the current after waiting 75 s, the time enough for the electrometer reading to stabilize after changing the voltage, and averaged the data acquired during the next 25 s. We chose

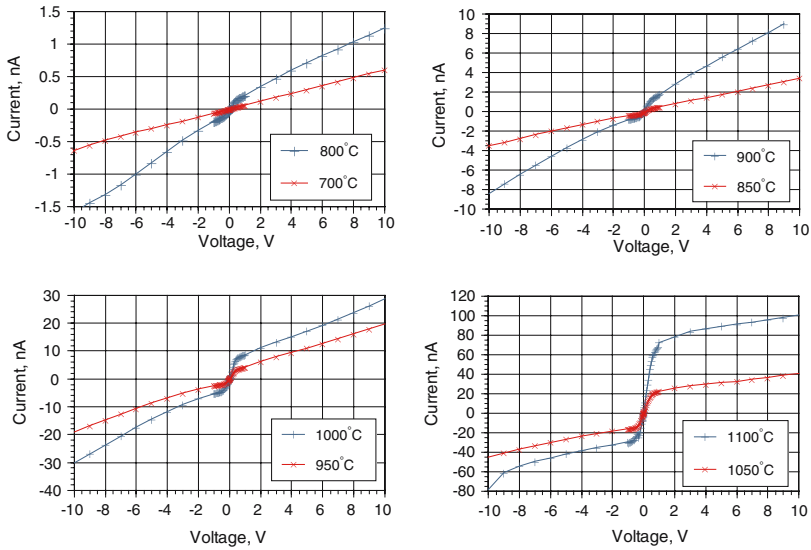


**Fig. 4** Measured  $I - V$  characteristics for a single fused-silica insulator suspended on two platinum wires, for temperatures in the range from 700 to 1,100°C

this relatively short measurement time considering the possibility of the deterioration of the silica when it was exposed to high temperatures. Indeed, while the measurements were fairly reproducible at lower temperatures, at 1,100°C, we found the quartz specimen deteriorated and the leakage current changed with time.

### 3.3 Results

Figure 4 shows the measured  $I - V$  characteristics for the two-wire specimen at eight different temperatures in the range from 700 to 1,100°C. All data have been corrected for the offset determined with 0 V applied to the specimen.

At 700°C, the  $I - V$  characteristic is almost linear. However, at 800°C and above, an S-shaped (sigmoid) non linearity emerges for voltages within  $\pm 1$  V, and becomes more marked as the temperature increases.

### 3.4 Analyses and Discussion on the Two-Wire Experiment

One of the key predictions of the Schottky-diode model was the presence of the sigmoid feature in the curves due to the nonlinear behavior of the diodes formed at the Pt–SiO<sub>2</sub> points of contact. In the simplest version of the model, which considers only the two diodes, the current  $I$  is related to the voltage by [8]

$$I = \frac{I_{s1} I_{s2} \left[ \exp\left(\frac{qV}{kT}\right) - 1 \right]}{I_{s1} \exp\left(\frac{qV}{kT}\right) + I_{s2}} \tag{1}$$

**Fig. 5** Equivalent circuit for the fused-silica disc supported by platinum lead wires

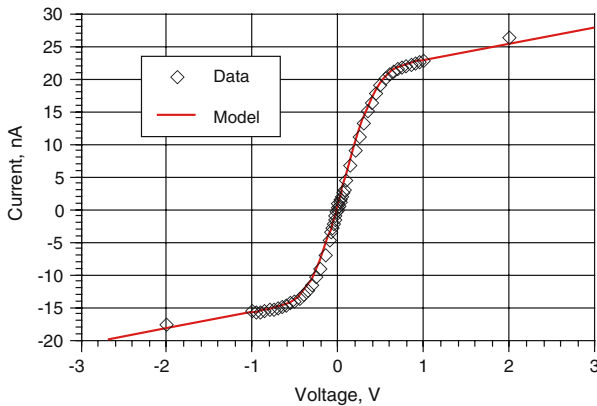
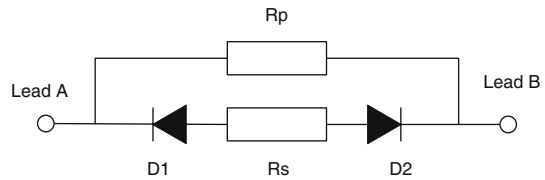


**Fig. 6** Expanded plot of the  $I - V$  characteristic at  $1,050^\circ\text{C}$  showing the nonlinear region and least-squares fit of the model to the data

where  $I_{s1}$  and  $I_{s2}$  are the saturation currents of the two diodes. This function has the expected sigmoid shape in the region within  $\pm 1$  V, and constant currents of  $I_{s1}$  and  $I_{s2}$  at voltages above and below this range. Note that the shape of the nonlinearity is completely determined by the parameter  $q/(kT)$ , and the only free parameters in the model are the saturation currents that determine the amplitude of the nonlinearity.

In addition to the sigmoid feature, the measured  $I - V$  characteristics also show a distinct ohmic behavior for voltages outside the  $\pm 1$  V range. We therefore included in the electrical model, Fig. 5, a series resistance between the two diodes to represent the bulk resistance within the fused silica insulator, and a resistance parallel to the diodes, which, we speculate might represent or include the surface conduction of the system. Figure 6 shows the leastsquares fit of the model to the measured characteristic for the insulator at  $1,050^\circ\text{C}$ .

Leastsquares fits were carried out for all the curves in Fig. 4. The saturation currents of the two diodes were determined from the fits and, as shown in Fig. 7, the saturation currents increased exponentially with the temperature. The two curves in Fig. 7 show the leastsquares fit of the measured saturation currents to the equation

$$I_s = -AT^2 \exp(-q\phi_b/kT), \quad (2)$$

which describes the current in a Schottky diode due to thermionic emission over a potential barrier of height  $q\phi_b$ . The parameter  $A$  is proportional to the contact area of the metal–semiconductor junction. The values of barrier height inferred from the



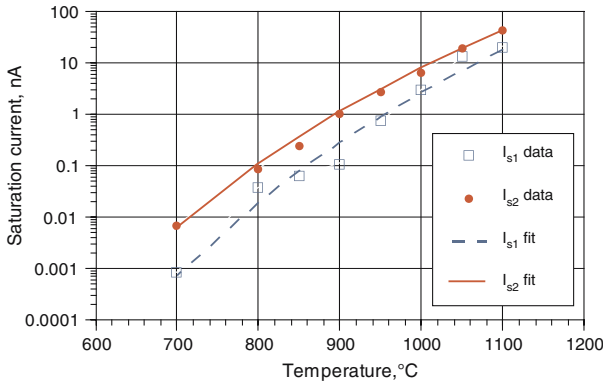


**Fig. 7** Saturation currents of the two diodes determined from fits to the model shown in Fig. 5, and the fit of the saturation currents to Eq. 2

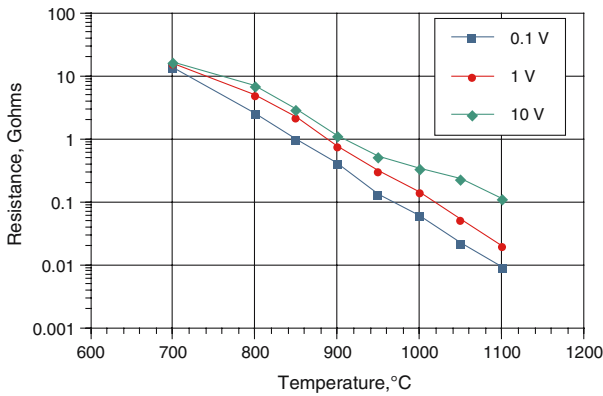


**Fig. 8** “Large-signal” measurements of the insulation resistance inferred from the data of Fig. 5, using excitation voltages of  $\pm 0.1$  V,  $\pm 1$  V, and  $\pm 10$  V

two sets of data of Fig. 7 are 2.7 and 3.1 eV. These values compare favorably with the values predicted from theory, ranging from 2.5 to 3.1 eV, for amorphous silica [8].

Figure 8 shows the resistance calculated from the  $I - V$  characteristics for each temperature using voltages of  $\pm 0.1$  V,  $\pm 1$  V, and  $\pm 10$  V. For  $700^\circ\text{C}$ , the three calculated resistance values are much the same since the  $I - V$  characteristic is linear. However, at higher temperatures, the diode behavior emerges in the  $I - V$  characteristics, and the discrepancies among the resistance measurements grow. Figures 6 and 8 show that measurements of the insulation resistance must be carried out with voltages below  $\pm 0.1$  V in order to avoid the nonlinearity effects, and prevent underestimates of the bias in temperature measurements.

The close match of both the observed nonlinear features of the  $I - V$  curves and the temperature dependence of the saturation currents to the theory, strongly support the hypothesis that Schottky-barrier diodes affect the properties of the insulation in SPRTs. However, the symmetry of the model means that these measurements cannot determine the polarity of the diodes.

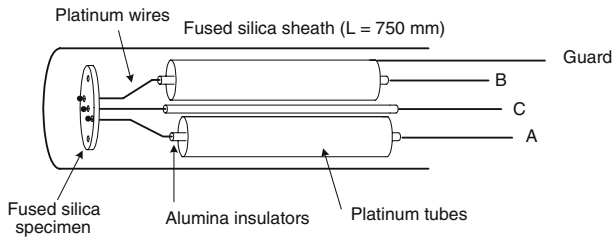


**Fig. 9** Structure of the specimen and holder for the three-wire experiment

## 4 Experiments to Determine Diode Polarity

### 4.1 Structure of the Specimen

Figure 9 shows the structure of the sample holder and specimen for the “three-wire” experiment to determine the polarity of the diodes. The basic structure is similar to that for the two-wire experiment, except that an additional lead wire has been included and contacted to the central hole of the fused-silica specimen. Leads A and C were connected to their voltage sources, respectively, Lead B was connected to the current meter, and the guard was connected to the guard point of the measurement circuit. The fused-silica disk and the air are from the same source as the specimen for the two-wire experiment.

### 4.2 Experimental Procedures

We prepared another Yokogawa Model 7651 programmable voltage source to apply the bias voltage to the central lead C. For each temperature setting, we first fixed  $V_C$  and swept  $V_A$ , from  $-10\text{ V}$  to  $10\text{ V}$  in the lower to higher sequence. For each voltage setting, we measured the current after waiting 75 s from changing the voltage, and averaged the data acquired during the next 25 s.

### 4.3 Results and Discussion

Figure 10 shows the results of the three-wire experiment carried out at  $1,000^\circ\text{C}$ . The key feature of the curves is that the current is almost independent of  $V_{AB}$  when the bias voltage  $V_C$  is negative. This shows that  $V_C$  has reverse-biased both diodes causing them to be in their high-resistance state and, hence, the polarity of the diodes is as shown in the equivalent circuits of Figs. 5 and 11; the metal being the anode and the fused silica being the cathode. The polarity of the Schottky-barrier diode formed by the contact of a metal and a semiconductor is determined by the majority carrier in the semiconductor [11]. The observations confirm that the fused silica behaves as a p-type semiconductor at high temperatures. Figure 10 also shows an upward kink near  $V_{AB} = +1$  to  $+3\text{ V}$  in the curves for  $V_C > 1\text{ V}$ ; we have no explanation for this effect.

The mechanism of reverse-biasing the diodes explains the enhancement of the insulation resistance observed by Berry [4] when a fifth (guard) wire is included in

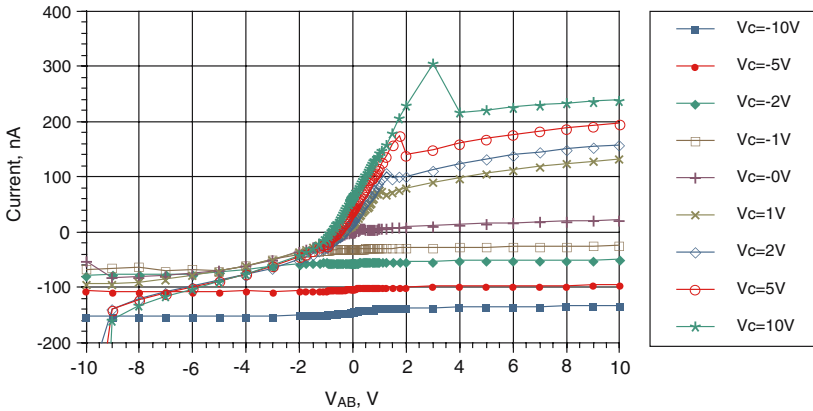


Fig. 10 Results of the three-wire experiment at 1,000°C

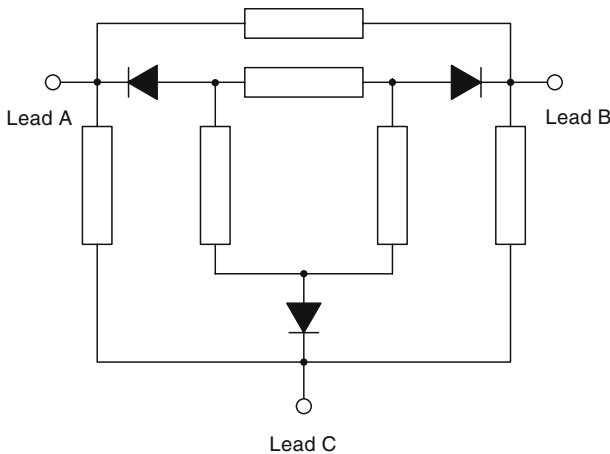


Fig. 11 Electrical model of the insulator with three wires

an SPRT assembly, and biased negatively with respect to the SPRT resistance measurement circuit. This mechanism opens up several possibilities for either improved SPRTs, or methods for assessing the insulation resistance effects in existing SPRTs. For example, Berry observed that a wire mesh outside the SPRT had a similar effect as the fifth wire. It may be that the graphite crucible of a fixed-point cell could be subjected to a bias voltage to achieve the same effect.

## 5 Discussion and Conclusions

### 5.1 Confirmation of the Schottky Diode Model

In this article, we investigated the nonlinear  $I - V$  characteristics of a single fused-silica insulator from an SPRT. The results from the “two-wire” experiment confirm

the existence of Schottky-barrier diodes formed at the points of contact between the platinum and silica, which is hypothesized in the accompanying article [8]. Both the observed non-linearity and the measured temperature dependence of the diode's saturation currents support the Schottky-barrier model.

The results from the “three-wire” experiment and the measured Schottky-barrier heights from the “two-wire” experiment confirm the polarity of the diodes: the metal is the anode and the fused silica is the cathode. This is consistent with the fused silica behaving as a p-type semiconductor at high temperatures.

Figure 5 shows a simple equivalent circuit for a single fused-silica disc supported by two platinum wires. The equivalent circuit suggests that there are three contributions to the insulation resistance of a fused silica insulator: (i) the nonlinear resistance of the two diodes, (ii) the bulk resistance of the fused silica, and (iii) a parallel conductance, perhaps due to surface conduction of the insulator. At temperatures below 750°C or so, the surface conductance part of the model dominates the behavior of the insulation resistance. At higher temperatures, the saturation current of the diodes rises exponentially, and causes the diodes to shunt the surface conductance, and thereby dominate the behavior at high temperatures.

## 5.2 Application of the Model to Uncertainty Assessment

It is hoped that this new model will enable the development of experiments to aid in the assessment of uncertainties in temperature measurements due to insulation breakdown. Berry, for example, noted that the quality of the SPRT insulation depended on the furnace power supplies and the grounding or otherwise of metal mesh around the SPRT. Re-investigation of Berry's observations, in light of the model presented in the accompanying article [8], and the observations of the three-wire experiment presented here, might point to a new method to assess the insulation resistance effects.

The model highlights potential problems in the direct measurement of the insulation resistance. The non-linearity of the diodes, which emerges at voltages above  $\pm 0.1$  V, means that measurements of resistance made using higher voltages will overestimate the resistance, and underestimate the resulting bias in temperature measurements.

## 5.3 Application to Improved SPRT Designs

The Schottky-barrier model should enable improved designs for SPRTs. Initially, now that the mechanism for the insulation breakdown has been identified, it may be possible to improve the design of the internal structure and insulators of the SPRTs to reduce the effects of the insulation breakdown. Alternatively, better quality materials, both insulators and wires, may be a solution.

The model also supports the observations of Berry and others that the insulation resistance can be enhanced through the use of the fifth (guard) wire connected to a bias voltage. This or similar methods may prove to be a viable means to overcome or assess SPRT insulation resistance effects.

**Acknowledgment** The authors thank Mr. Y. Kamiyama of Chino Corporation for providing the quartz disk specimen and the related information used in this test.

## References

1. X. Li, J. Zhang, J. Su, D. Chen, *Metrologia* **18**, 203 (1982)
2. J.P. Evans, *J. Res. Natl. Bur. Stand. (U.S.)* **89**, 349 (1984)
3. J. Zhang, R.J. Berry, *Metrologia* **21**, 207 (1985)
4. R.J. Berry, *Metrologia* **32**, 11 (1995)
5. K. Yamazawa, M. Arai, in *Temperature, Its Measurement and Control in Science and Industry*, vol. 7, ed. by D.C. Ripple (AIP, New York, 2003), pp. 363–368
6. N.P. Moiseeva, in *Proc. Tempmeko 2004, 9th International Symposium on Temperature and Thermal Measurements in Industry and Science*, ed. by D. Zvizdic (FSB/LPM, Zagreb, Croatia, 2004), pp. 433–438
7. N.P. Moiseeva, A.I. Pokhodun, B.W. Mangum, G.F. Strouse, *Proc. Tempmeko 1999, 7th International Symposium on Temperature and Thermal Measurements in Industry and Science*, (Edaaw Johannissen bv, Delft, 1999), pp. 371–376
8. D.R. White, M. Arai, A. Bittar, K. Yamazawa, A Schottky-Diode Model of the Non-linear Insulation Resistance Effects in SPRTs - Part I: Theory, in *Proceedings of TEMPMEKO 2007* (to be published in *Int. J. Thermophys.*)
9. K. Yamazawa, M. Arai, in *Proceedings TEMPMEKO 2001, 8th International Symposium on Temperature and Thermal Measurements in Industry and Science*, ed. By B. Fellmuth, J. Seidel, G. Schol (VDE Verlag, Berlin, 2002), pp. 115–120
10. *Private communication with the supplier*
11. S.M. Sze, *Physics of Semiconductor Devices*, 2nd edn. (John Wiley & Sons, New York, 1981)